TWQH Attitude Control Experiments on Horizon Ground Simulator and Flight Test

Stefan Eugen STOIAN[1], Dragos Daniel ION-GUTA[1], Sandra Elena NICHIFOR*,[1], Florentin SPERLEA[1], Achim IONITA[1]

*Corresponding author
[1]INCAS – National Institute for Aerospace Research "Elie Carafoli",
B-dul Iuliu Maniu 220, Bucharest 061126, Romania,
stoian.stefan@incas.ro, guta.dragos@incas.ro, nichifor.sandra@incas.ro*,
sperlea.florentin@incas.ro, ionita.achim@incas.ro

DOI: 10.13111/2066-8201.2020.12.1.18

Received: 10 January 2020/ Accepted: 14 February 2020/ Published: March 2020

Abstract: *This paper presents the results of two experiments on the Horizon ground simulator and outdoor flight test of TWQH hybrid UAV in presence of wind perturbation. The simulation results show the stability and error boundedness of the PID controller while the experimental inflight tests indicate the good performances of the proposed controller.*

Key Words: *hybrid UAV, hover, attitude control, flight test, stability, PID regulator*

NOTATIONS

m [kg]	mass
I_{xx}, I_{yy}, I_{zz} [kgm^2]	main inertial moments
I_r [kgm^2]	rotor moment of inertia
Ω_r [rad/sec]	engine rotation
c_f [N/(rad/sec)^2]	strength coefficient
c_m [Nm/(rad/sec)^2]	moment coefficient
g [m/sec^2]	gravitational acceleration
ρ [kg/m^3]	density of air
a,b,c [m]	distances between rotors and center of gravity
p,q,r [rad/sec]	angular velocities
$\dot{p}$, $\dot{q}$, $\dot{r}$ [rad/sec^2]	angular accelerations
φ, θ, ψ [rad]	Euler angles
$\dot{\varphi}$, $\dot{\theta}$, $\dot{\psi}$ [rad/sec]	angular velocities
U_1, U_2, U_3, U_4 [N]	command variables
Δx [m]	variation of the distance on the Ox axis
Δy [m]	variation of the distance on the Oy axis
Δz [m]	variation of altitude
$\overline{M_T}$	moment vector due to thrust
$\overline{h_r}$	giroscopic moment due to rotors
w [m/sec]	translational velocity in body axis on the Oz axis

$\bar{V}$	velocity vector on the Oxyz frame
$\overline{F_T}$	forces vector to thrust
$\overline{F_G}$	gravitional vector
$\bar{x}$	position vector on the Oxyz frame
$\bar{X}$	position vector on the Exyz frame
C	rotation matrix
$\bar{B}$	transformation matrix for angluar velocities

ACRONYMS

TWQH	Hybrid Tandem Wing quadrotor H
QH	Quadrotor H Configuration
UAV	Unmanned Aerial Vehicle
PID	Proportional-Integral-Derivative control
CoM	Center of Mass
GPS	Global Position Sytem

1. INTRODUCTION

The TWQH configuration is an alternative for diversifying and extending the different missions specific to UAV vehicles (border patrol, search, fire monitoring and road traffic). The TWQH vehicles offer a way to execute the flight phases specific both to fixed wing vehicles (long distance, tracking, monitoring, identification) and rotary wing vehicles (hovering, VTOL, monitoring, identification). The TWQH is equipped with all necessary sensors and actuators for fully autonomous operations. The QH configuration is still an under-actuated, non-linear coupled system in spite of the four rotors. The gyroscopic effect and coupled properties of this two scale dynamics need a inner-loop and outer-loop gains to guarantee the closed loop stability of TWQH vehicle [1]. The goal of this work is to stabilise the QH states in hover. Prior to PID control algorithm implementation it must be tested in HORIZON ground simulator. The paper presents the results of numerical simulations in the HORIZON^{mp} simulation environment of TWQH hybrid platform dynamics as well as in-flight tests for fixed point flight (hover). These simulations and tests provide an image in a first stage of the stability and control characteristics in order to improve the performance of the platform dynamics. The QH dynamics includes a PID regulator for controlling altitude and pitch, roll and rotational attitudes.

2. TWQH DYNAMIC MODELLING

The mathematical model for a UAV vehicle type TWQH with four quadcopter propellers and an airplane propeller is indispensable in simulating the vehicle movement and later in modeling the control algorithms. The purpose of this chapter is to describe the vehicle behavior with satisfactory accuracy. With some improvements the research discussed in this chapter could also serve as the basis for future developments. VTOL QH configuration considered that open-loop system has a natural instability. A flight control system capable of stabilizing the attitude is quite challenging. The motion equations for the TWQH configuration are those applied in flight mechanics which are detailed in the works of Etkin [2], Roskam [3], Hacker [4] applied to a UAV vehicle where the traction vector includes the fixed wing component such as the rotary wing component.

The mathematical model describes TWQH movement and behavior with respect to the initial input values of the model and external influences on vehicle. By using mathematical model it is possible to estimate the attitude and vertical position of the QH configuration by knowing the four angular velocities of propellers. TWQH frame with QH propellers are the components that will be taken into account in this dynamics. TWQH design with corresponding angular velocities for QH configuration is presented in fig. 1.

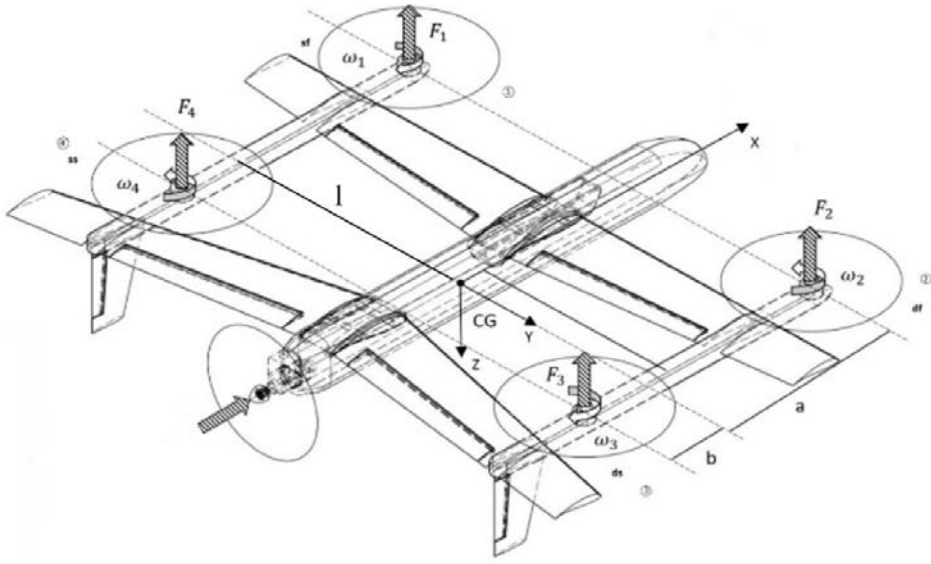

Figure 1. TWQH Configuration

The orientation of the plane axis system (Body axis) in relation to the reference system related to the Earth is as follows : Ox axis, forward, Oy axis, to the right and Oz axis, down.

The model developed in this paper assumes the following:

- The TWQH structure is rigid. Then the QH nonlinear dynamics can be derived by using Newton – Euler formulas;
- The TWQH structure is supposed symmetrical;
- The CoM of TW configuration and QH configuration in body fixed frame are assumed to coincide;
- Thrust components are proportional to the square of the propeller speed;
- The QH model should consider the gravity force, gyroscopic moment and the change in speed effects of the rotary propeller. The QH model should take into account the gravity, gyroscope and change of speed effects of the rotary propeller. Aerodynamic forces and moments can be ignored at low speeds (hover phase). The contributions of atmospheric disturbances (wind, atmospheric turbulence, burst) have been introduced according to [5]. Let Oxyz be a body-fixed frame whose origin O is at the center of mass (CoM). The absolute position of QH is defined by position (x, y, z) and the attitude defined by the Euler angles. QH dynamics uses Newton – Euler method expressed by differential equations as follows:

$$m(\dot{\overline{V}} + skew(\Omega) \cdot \overline{V}) = \overline{F_G} + \overline{F_T} \tag{1}$$

$$\dot{\overline{x}} = C\overline{\mathrm{V}} \tag{2}$$

$$I\dot{\overline{\Omega}} + \dot{\overline{h_r}} + skew(\Omega)\left(I \cdot \overline{\Omega} + \overline{h_r}\right) = \overline{M_T} \tag{3}$$

$$\dot{\overline{\omega}} = B^{-1}\overline{\Omega} \tag{4}$$

where components are defined as follows:

$$\bar{V} = \begin{pmatrix} u \\ v \\ w \end{pmatrix} \quad \overline{F_G} = C \cdot \begin{pmatrix} 0 \\ 0 \\ mg \end{pmatrix} \quad \overline{F_T} = \begin{pmatrix} 0 \\ 0 \\ U_1 \end{pmatrix} \quad \bar{x} = \begin{pmatrix} x \\ y \\ z \end{pmatrix} \tag{5}$$

$$\overline{\Omega} = \begin{pmatrix} p \\ q \\ r \end{pmatrix} \quad \overline{\omega} = \begin{pmatrix} \varphi \\ \theta \\ \psi \end{pmatrix} \quad skew(\Omega) = \begin{pmatrix} 0 & -r & q \\ r & 0 & -p \\ -q & p & 0 \end{pmatrix} \tag{6}$$

$$\overline{M_T} = \begin{pmatrix} U_2 \\ U_3 \\ U_4 \end{pmatrix} \quad \overline{h_r} = \begin{pmatrix} h_{rx} \\ h_{ry} \\ h_{rz} \end{pmatrix} \quad I = \begin{pmatrix} I_{xx} & 0 & 0 \\ 0 & I_{yy} & 0 \\ 0 & 0 & I_{zz} \end{pmatrix} \tag{7}$$

$$C = \begin{pmatrix} \cos\psi\cos\theta & \sin\psi\cos\theta & -\sin\theta \\ \sin\varphi\sin\theta\cos\psi - \cos\varphi\sin\psi & \sin\varphi\sin\theta\sin\psi + \cos\varphi\cos\psi & \sin\varphi\cos\theta \\ \cos\varphi\sin\theta\cos\psi + \sin\varphi\sin\psi & \cos\varphi\sin\theta\sin\psi - \sin\varphi\cos\psi & \cos\varphi\cos\theta \end{pmatrix} \tag{8}$$

$$B = \begin{pmatrix} 1 & 0 & -\sin\theta \\ 0 & \cos\varphi & \cos\theta\sin\varphi \\ 0 & -\sin\varphi & \cos\theta\cos\varphi \end{pmatrix} \tag{9}$$

The system that defines the movement of the quadcopter includes the following states and control variables:

- The state variables are: (u, v, w, p, q, r, φ, θ, ψ, x, y, z)
- The control variables are: (U_1, U_2, U_3, U_4)

The gyroscopic effect due to the propulsion group rotation is kept only for the Oz axe (Oxz plane is a plane of symetry):

$$h_{rx} = 0, h_{ry} = 0 \text{ and } h_{rz} \neq 0 \tag{10}$$

To define the trajectory parameters, it is necessary to introduce a Earthfixed frame E(X,Y,Z). Eqtions (1) and (2) can be expressed as:

$$m\dot{\bar{X}} = \overline{F_G} - \overline{F_T}C_3 \tag{11}$$

$$\dot{\bar{X}} = C^T\overline{V} \tag{12}$$

The nonlinear system can be rewritten in the new state space form with states variables and control vector

- The state variables are: $(\dot{X}, \dot{Y}, \dot{Z}$, p, q, r, φ, θ, ψ, X, Y, Z)
- The control variables are: (U_1, U_2, U_3, U_4)

as follow:

$$\ddot{X} = -i_1U_1(cos\phi sin\theta cos\psi + sin\phi sin\psi) \tag{13}$$

$$\ddot{Y} = -i_1U_1(cos\phi sin\theta sin\psi - sin\phi cos\psi) \tag{14}$$

$$\ddot{Z} = g - i_1U_1(cos\phi cos\theta) \tag{15}$$

$$\dot{p} = i_5qr - qh_{rz} + i_2U_2 \tag{16}$$

$$\dot{q} = i_6rp + ph_{rz} + i_3U_3 \tag{17}$$

$$\dot{r} = i_7pq + i_4U_4 \tag{18}$$

$$\dot{\varphi} = p + qsin\varphi tan\theta + rtan\theta cos\varphi \tag{19}$$

$$\dot{\theta} = qcos\varphi - rsin\varphi \tag{20}$$

$$\dot{\psi} = q\frac{sin\varphi}{cos\theta} + r\frac{cos\varphi}{cos\theta} \tag{21}$$

$$\dot{X} = \mathrm{u}\cos\psi\cos\theta + v\,(\sin\varphi\sin\theta\cos\psi - \cos\varphi\sin\psi) + w\,(\cos\varphi\sin\theta\cos\psi + \sin\varphi\sin\psi) \tag{22}$$

$$\dot{Y} = u\sin\psi\cos\theta + v(\sin\varphi\sin\theta\sin\psi + \cos\varphi\cos\psi) + w\,(\cos\varphi\sin\theta\sin\psi - \sin\varphi\cos\psi) \tag{23}$$

$$\dot{Z} = -usin\theta + v\sin\varphi\cos\theta + w\cos\varphi\cos\theta \tag{24}$$

where:

$$h_{rz} = I_r\Omega_r \tag{25}$$

$$\Omega_r = (\omega_1 - \omega_2 + \omega_3 - \omega_4) \tag{26}$$

The following notations are made:

$$i_1 = \frac{1}{m};\ i_2 = \frac{1}{I_{xx}};\ i_3 = \frac{1}{I_{yy}};\ i_4 = \frac{1}{I_{zz}};\ i_5 = \frac{I_{yy}-I_{zz}}{I_{xx}}; \tag{27}$$

$$i_6 = \frac{I_{zz}-I_{xx}}{I_{yy}};\ i_7 = \frac{I_{xx}-I_{yy}}{I_{zz}};\ i_8 = \frac{I_r\Omega_r}{I_{xx}};\ i_9 = \frac{I_r\Omega_r}{I_{yy}}; \tag{28}$$

Total thrust produced by the four rotors in free air is:

$$U_1 = c_f(\omega_1^2 + \omega_2^2 + \omega_3^2 + \omega_4^2) \tag{29}$$

Control torque with respect to Oxyz frame generated by the four rotors is:

$$U_2 = c_f l(\omega_1^2 - \omega_2^2 - \omega_3^2 + \omega_4^2) \tag{30}$$

$$U_3 = c_f[a(\omega_1^2 + \omega_2^2) - b(\omega_3^2 + \omega_4^2)] \tag{31}$$

$$U_4 = c_M(\omega_1^2 - \omega_2^2 + \omega_3^2 - \omega_4^2) \tag{32}$$

Inverted movement matrix for rotor speeds is used for calculation of squared angular propeller's velocities that input variables as follows:

$$\begin{pmatrix}\omega_1^2\\ \omega_2^2\\ \omega_3^2\\ \omega_4^2\end{pmatrix} = \frac{1}{4(a+b)}\begin{pmatrix}\frac{2b}{c_f} & \frac{a+b}{c_f l} & \frac{2}{c_f} & \frac{a+b}{c_m}\\ \frac{2b}{c_f} & -\frac{a+b}{c_f l} & \frac{2b}{c_f} & -\frac{a+b}{c_m}\\ \frac{2a}{c_f} & -\frac{a+b}{c_f l} & -\frac{2}{c_f} & \frac{a+b}{c_m}\\ \frac{2a}{c_f} & \frac{a+b}{c_f l} & -\frac{2}{c_f} & -\frac{a+b}{c_m}\end{pmatrix}\begin{pmatrix}U_1\\ U_2\\ U_3\\ U_4\end{pmatrix} \tag{33}$$

The hybrid vehicle design called TWQH (Twin Wing Quadrotor H) configuration was carried out with the AAA program [6] including: main dimensions, gravimetric and inertial characteristics, aerodynamic characteristic angles, propulsion and equipment. Calculations and results regarding the performance and stability characteristics (depreciation, frequencies, time constants, overshoot, settling time) are based on the regulations of specifications MIL 8785 [7], MIL STD 1797 [8] and ADS - 33 PRF [9] as well as from the specific rules UAV - STANAG 4703[10]. The data and parameters used only in the QH configuration are presented below:

$m = 36\,kg,\ I_{xx} = 3.36\,kgm^2,\ I_{yy} = 9.88\,kgm^2,\ I_{zz} = 12.35\,kgm^2\ \ I_r = 0.007\,kgm^2,$
$\Omega_r = 345 \ldots 690\,rad/sec,\ c_f = 0.00076\,N/(\frac{rad}{sec})^2,\ c_m = 0.0000112\,Nm/(\frac{rad}{sec})^2$
$a = 0.57\,m,\ b = 0.67\,m,\ l = 1.1\,m.$

3. HORIZON GROUND CONTROL SIMULATOR

The HORIZON ground control simulator [11] is a state-of-the-art modelling and analysis software packages who use UAVs preconfigured with a MicroPilot autopilot [12]. It can track the flight path using a moving map display which monitors the aircraft status and flight conditions. The HORIZON^{mp} is also a computer interface to the autopilot that manages the transmission of the flight plans, and records telemetry and sensor data. The developers use HORIZON^{mp} to set up the autopilot for the aircraft in which it is installed and to design flight plans. The HORIZON^{mp} Video window can give a view and save video streams and save video frames as bitmap images. The MicroPilot Autopilot gives also support to install, configure, tune PID loops and operate MP2128 autopilot in our TWQH multirotor vehicle. The users must have a previously knowledge of the UAVmodel, mechanics and flight dynamics. The HORIZON^{mp} window is a visual interface of the autopilot. The aircraft can be tracked by displaying the moving map and monitoring the status and sensors of the aircraft. HORIZON^{mp} is also the physical interface of the autopilot. Files of settings and flight files can be sent to the autopilot via HORIZON^{mp}. Through a pair of radio modems, telemetry is received from the autopilot, flight points are transmitted to the aircraft and the payloads are monitored. HORIZON^{mp} can simulate flight path, wind conditions and radio and engine malfunctions. A flight simulation allows to check if the reference points chosen are correct and running simulations is a way to learn how to use HORIZON^{mp}. By running a simulation, it can be observed the operation of the take-off, landing and holding patterns that are part of the mission file. Most commercial implementations use a form of PID controller. Given the reference order and current status estimates, the PID parameters at each level can be estimated first offline (through modeling and simulation) to obtain a viable control law and fine tuning (in-flight) during the flight. The preference for the traditional PID controller is due to the ease of implementation on small UAV platforms and the simplicity of the end-user tuning process. However, PID controllers have limitations in terms of optimality and robustness. In addition, the tuning process becomes difficult if the UAV configuration differs from the one for which the controller was designed. All feedback loops are not in use at the same time. The MP2128HELI2 [12] enables feedback loops as required to control different aspects of flight. While the standard loops are easier to adjust, to achieve better performance in the (inner) attitude loops, the Rate loops are activated. These new speed loops are: • "Aileron from Roll Rate"/ "Roll Rate from Roll Roll" • "Elevator from Pitch Rate"/ "Rate Pitch from Pitch Error" • "Time from Yaw Rate"/ "Yaw Rate From Yaw Error". Because the MicroPilot autopilot controller is preconfigured for several UAV fixed-wing/rotary-wing vehicles the "Aileron, Elevator and Rudder" controls means in our QH configuration U_2, U_3, U_4 controls. The MicroPilot autopilot has possibility to fly a multirotor with several flight contol modes. In case QH configuration we adopt for hover the "CIC (Computer in Control) Position Arcade Mode". The Arcade mode is a set of control mode which allows a pilot to control a multirotor high level behavior without having to actually fly the multirotor. The option to use I terms of the PID in 400 Hz motor control loops improves performance and response to disturbances. It is suggested to use a low-pass filter on the gyro-rates (cutoff frequency with 20/30 Hz). The rate loop structure is set up as shown in figure 2:

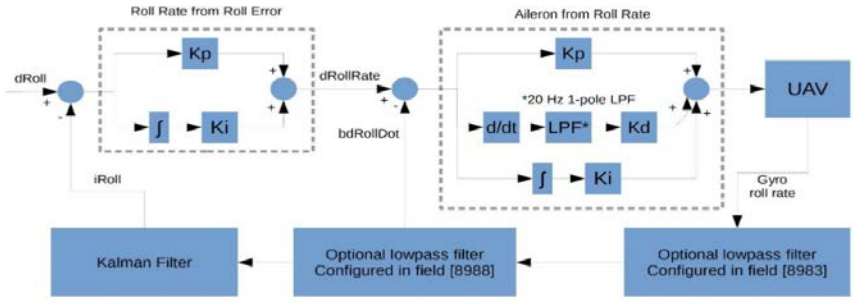

Figure 2. Rate loop diagram [12]

The "Hover Position Hold Mode using Rate Loops" is presented in fig. 3. The CIC Hover mode permits to hold the GPS position. In order to keep a position to hover waypoint the autopilot commands a desired velocity to move towards the waypoint and calculates the desired pitch and roll from error between the desired and command X and Y body velocities. In this type of subset of CIC mode, the stick inputs command either a rate of change proportional to the stick deflection or an absolute position. It is worth mentioning that all of the CIC arcade modes can be controlled by the RC transmitter joysticks.

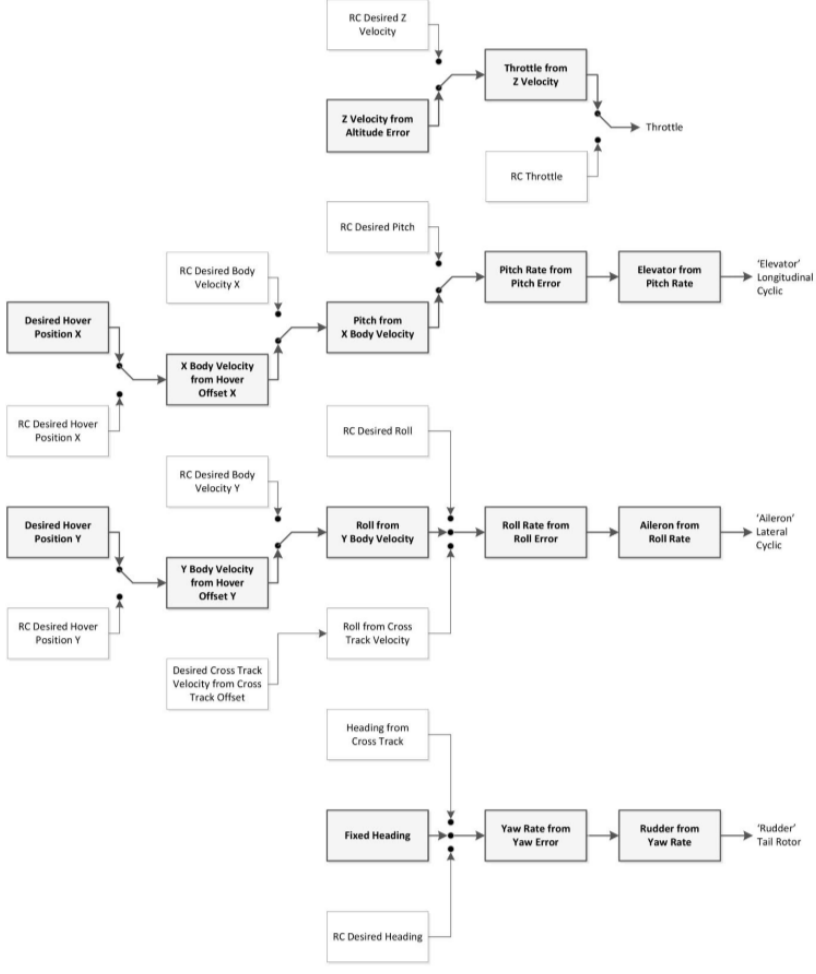

Figure 3. Hover Position Hold Mode using Rate Loops [12]

4. STABILIZATION OF TWQH IN ATTITUDE

Altitude and attitude controlled QH model is used for the control algorithm testing on experimental simulator before inflight tests.

Also, for the control model, it is important to be relatively easy to modify and implement on the inflight demonstrator. QH control system is split into inner and outer control loops because the QH configuration is under actuated system which does not allow direct control of all degrees of freedom. The inner loop controls the attitude angles together with the altitude position control.

The control algorithm as input has sensor data or calculated data from the dynamic model and reference data. The outputs of the control algorithm are the angular velocities of propellers, which can be translated to the pulse-with-modulation (PWM) signals.

To stabilise the QH configuration a PID controller is utilised [13-18]. The advantage of the PID controller is its simple structure and easy implementation. The well-known used form of the PID controller is:

$$e(t) = x_d(t) - x(t) \tag{34}$$

$$u(t) = K_p e(t) + K_d \frac{de(t)}{dt} + K_i \int_0^t e(\tau)d\tau \tag{35}$$

where $x_d(t)$, $x(t)$ are the desired and present states, e(t) is the difference between the desired state and the present state, u(t) is the control input and K_p, K_i and K_d are the proportional, integral and derivative parameters of the PID controller.

Here the PID controller for QH is specified for the altitude and attitude in a condensed form as follows:

$$U_i = \sum_{j=1}^{2}(K_p^j e_j(t) + K_d^j \frac{de_j(t)}{dt} + K_i^j \int_0^t e_j(\tau)d\tau) \tag{36}$$

where:

for altitude control	i=1	j=z,$\dot{Z}$
for roll control	i=2	j=φ, p
for pitch control	i=3	j=θ, q
for yaw control	i=4	j=ψ, r

The real angular velocities of rotors ω_i can be calculated from equation 33 with values from equation 29-32.

The performances of PID controller are tested in HORIZON^{mp} simulator by simulating stabilization of QH and they are verified in flight tests for hover phase.

Because the controller is more complex to achieve better performance in the inner loop, the rate loops block is considered (fig. 3).

5. SIMULATIONS AND INFLIGHT EXPERIMENTS

In order to validate the proposed controller developed in the previous chapter, we performed several simulation experiments using HORIZON ground simulator and in flight tests on the real TWQH, respectively.

5.1 HORIZON^{mp} simulation

We performed several simulations to verify that the proposed controller is able to stabilize the system in quite atmosphere and in presence of the wind perturbation.

The altitude was fixed at H=15 m and the hybrid platform maintened the stabilized hover.

a) Hover in quiet atmosphere - sudden orders (impulse) were given on the pitch command (front / back) and separately on the roll command (left / right). The response in pitch and roll axes are depicted in fig. 4.

The following response time values for pitch and roll were obtained:

- Pitch: t = 3,8 s for the first signal and t = 6,5 s for the second signal
- Roll: t = 4,15 s for the first signal and t = 4,06 s for the second signal

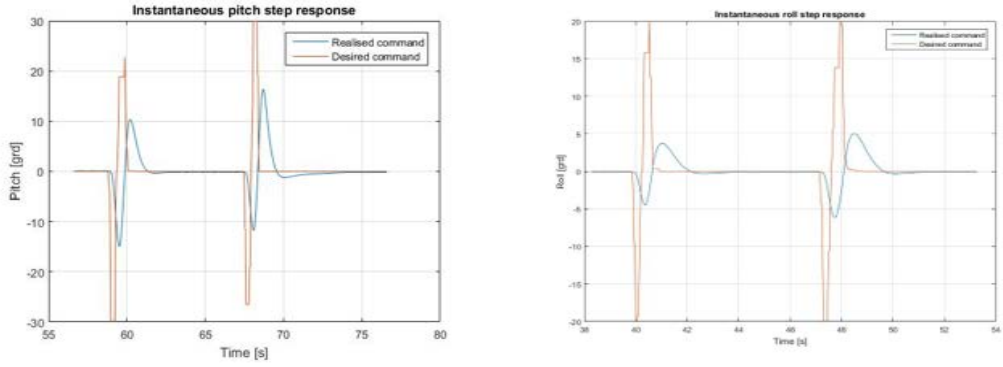

Figure 4. Instant response for pitch and roll

b) Hover in presence of wind (5 m/sec) from ahead (0º angle) At the height of H = 15m, the hybrid platform is turned and stopped in yaw at 55º, 90º and 180º angles until stabilization is achieved. Figure 5 depicts the altitude and the heading angle respone for the yaw input.

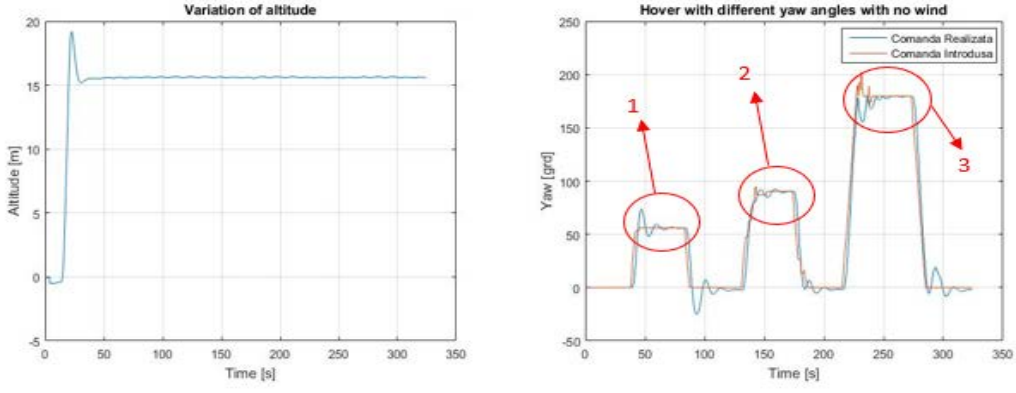

Figure 5. Hover in wind at 0º

The following oscillatory response values were obtained:

- Turning order at 55º (see figure 5, indicator 1) Period T = 12,13 s
  Frequency ω = 0,5179 rad/s
  Damping ξ = 0,2151
  Stabilization time t = 38,7 s
- Turning order at 90º (see figure 5, indicator 2) Period T = 10,5 s
  Frequency ω = 0,5984 rad/s
  Damping ξ is not conclusive
  Stabilization time t = 31,6 s
- Turning order at 180º (see figure 5, indicator 3) Period T = 6,7 s
  Frequency ω = 0,9378 rad/s

Damping ξ = 0,0022
Stabilization time t = 44,69 s

c) Hover in presence of wind (5 m/sec) at 45° angle

At the height of H = 15m the hybrid platform is turned and stopped in yaw at 55°, 90° and 180° angles until stabilization is achieved. Figure 6 depicts the altitude and the heading angle respone for the yaw input.

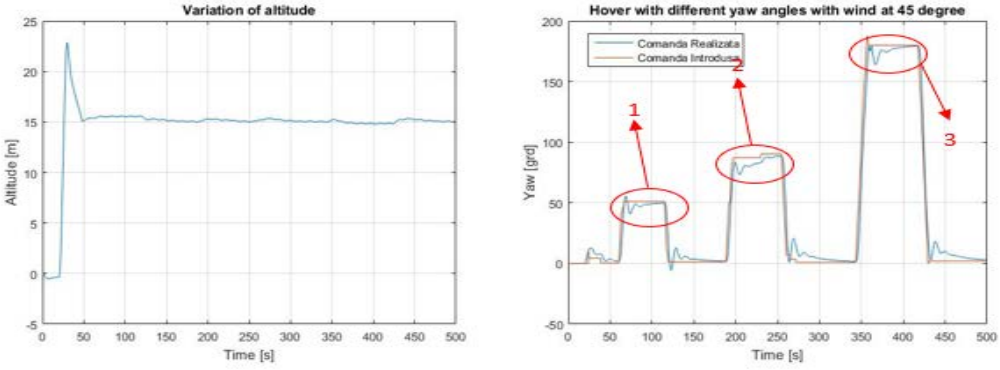

Figure 6. Hover in wind at 45°

The following oscillatory response values were obtained:

- Turning order at 55° (see figure 6, indicator 1) Period T = 11,27 s
  Frequency ω = 0,5575 rad/s
  Damping ξ = 0,338
  Stabilization time t = 47,95 s
- Turning order at 90° (see figure 6, indicator 2) Period T = 10,5 s
  Frequency ω = 0,5984 rad/s
  Damping ξ = 0,035
  Stabilization time t = 57,70 s
- Turning order at 180° (see figure 6, indicator 3) Period T = 7 s
  Frequency ω = 0,8976 rad/s
  Damping ξ = 0,0213
  Stabilization time t = 61,64 s

d) Hover in presence of wind (5 m/sec) at 90° angle

At the height of H = 15m the hybrid platform is turned and stopped in yaw at 55°, 90° and 180° angles until stabilization is achieved. Figure 7 depicts the altitude and the heading angle respone for the yaw input.

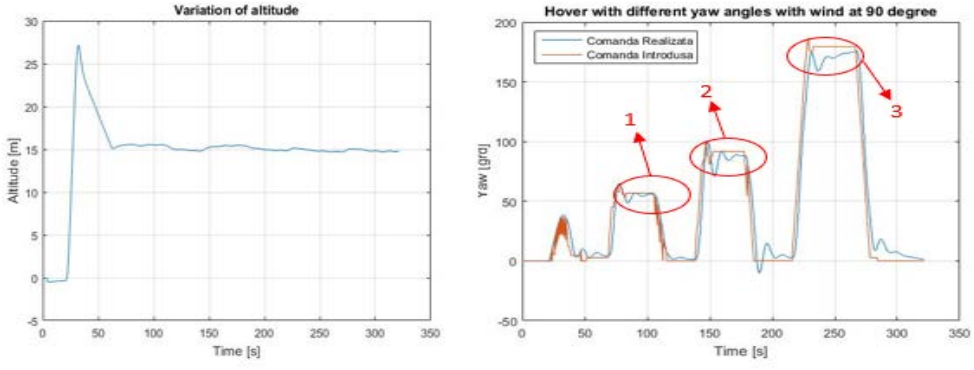

Figure 7. Hover in wind at 90°

The following oscillatory response values were obtained:

- Turning order at 55º (see figure 7, indicator 1) Period T = 11,97 s
  Frequency ω = 0,5249 rad/s
  Damping ξ = 0,1348
  Stabilization time t = 30,46 s
- Turning order at 90º (see figure 7, indicator 2) Period T = 9,5 s
  Frequency ω = 0,6614 rad/s
  Damping ξ = 0,0810
  Stabilization time t = 31,45 s
- Turning order at 180º (see figure 7, indicator 3) Period T = 6,1 s
  Frequency ω = 1,0300 rad/s
  Damping ξ = 0,0197
  Stabilization time t = 38,75 s

The responses to an attitude controls input are as follows:

- the movement stabilizes in about 30 - 60 sec.,
- the oscillations have a period of approx. 10-12 sec., frequencies of 0.52 - 0.96 rad / sec and slow damping of the order 0.02 - 0.34. The depreciation decreases as the rotation order increases.
- the response time to a roll or pitch command is 4-6.5 sec.

5.2 Flight test simulation

The data recorded from the in-flight experiments that are analyzed below are the response in time of the fixed-point positions, the angular attitudes (roll, pitch and rotation) as well as the forces on each rotor and the associated angular speeds.

The flights were conducted in a perturbed atmosphere (wind variations of about 3-5 m/s).

a) Flight nr. 164404 from 23.04.2019

For 12 seconds, the position deviations in meters were recorded (fig. 8), as well as the response in roll and pitch (fig. 9, 10).

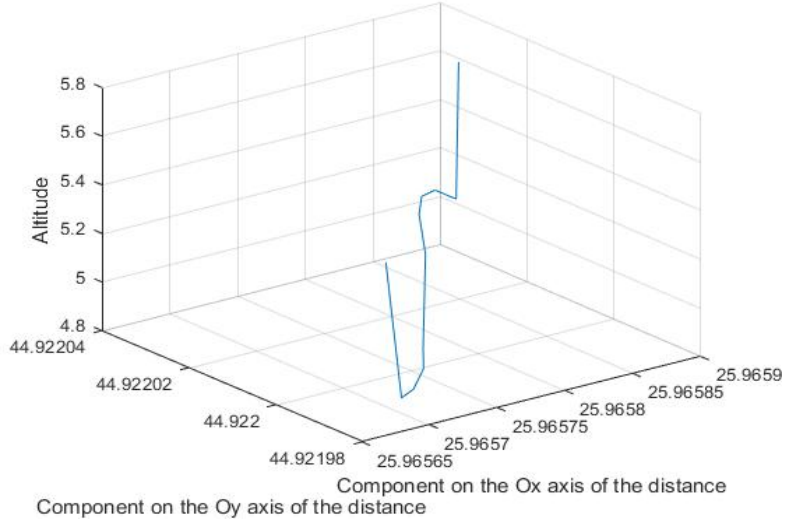

$\Delta x = 0{,}00018$ m

$\Delta y = 0{,}001882$m

$\Delta z = 0{,}91$m

Figure 8. Trajectory simulation case 1

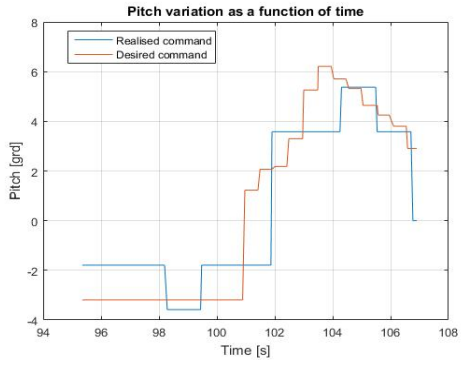

Figure 9. Pitch variation as a function of time

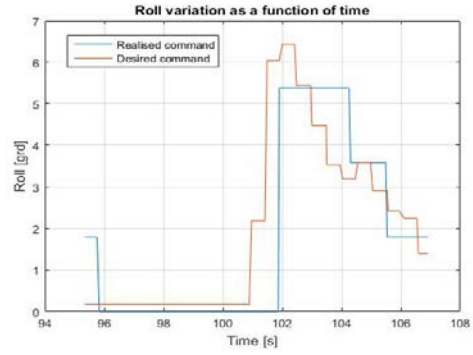

Figure 10. Roll variation as a function of time

The estimated delays in response to a pitch and roll command are as follows: T_{pitch} = 0,0939 and T_{roll} = 0,093 s.

The percent values of the forces on each rotor were extracted from the database being shown in Fig. 11-14.

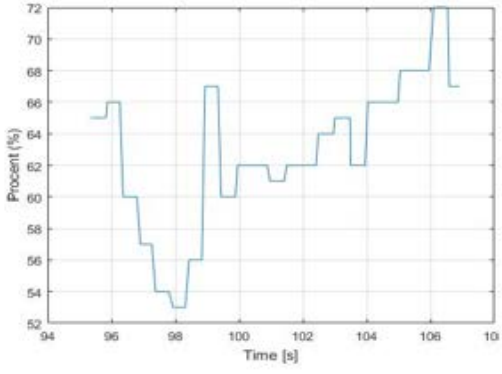

Figure 11. Rotor control force 1

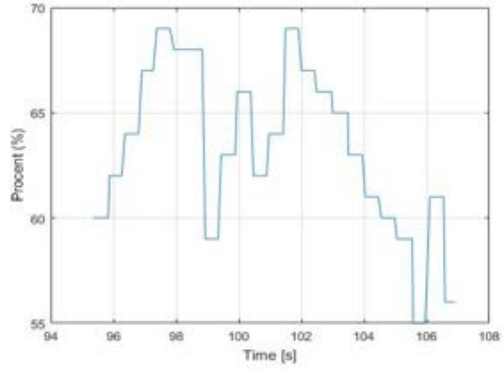

Figure 12. Rotor control force 2

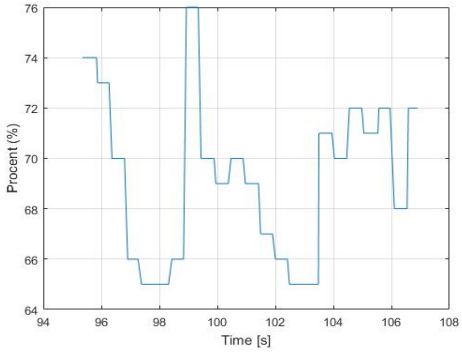

Figure 13. Rotor control force 3

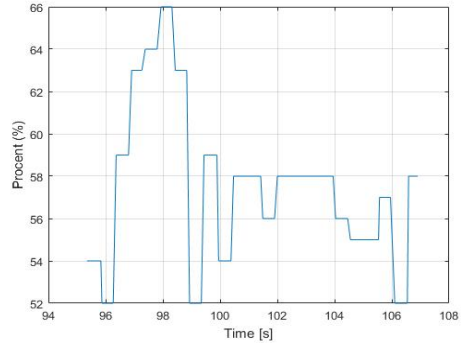

Figure 14. Rotor control force 4

b) Flight nr. 194818 from 18.04.2019

For 10 seconds, the position deviations in meters were recorded (fig. 15), as well as the response in roll and pitch (fig. 16, 17).

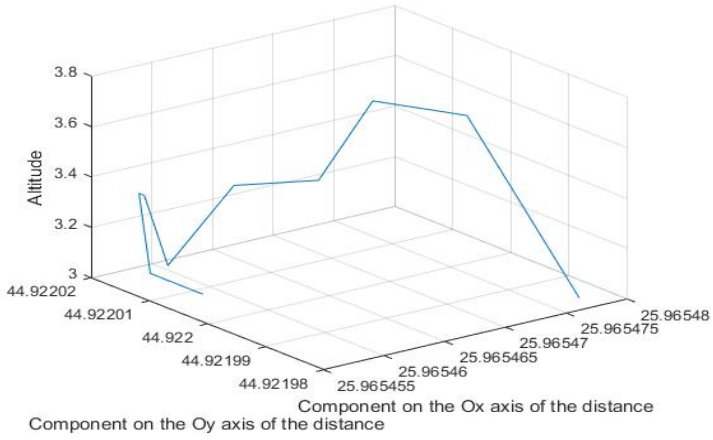

$\Delta x = 0{,}000026\text{m}$

$\Delta y = 0{,}000012\text{m}$

$\Delta z = 3{,}62\text{m}$

Figure 15. Trajectory simulation case 2

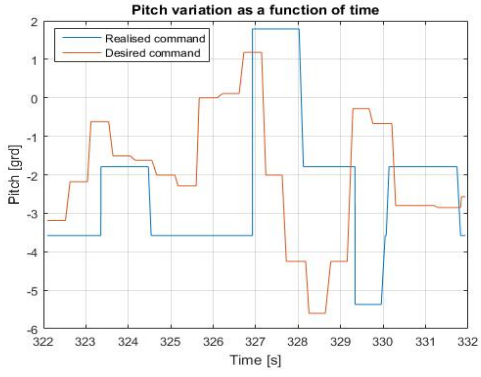

Figure 16. Pitch variation as a function of time

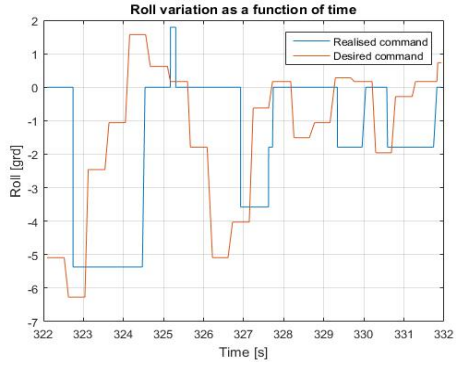

Figure 17. Roll variation as a function of time

The estimated delays in response to a pitch and roll commands are as follows: $T_{pitch} = 0{,}09$ s and $T_{roll} = 0{,}08$ s.

The percent values of the forces on each rotor were extracted from the database being shown in Fig. 18-21.

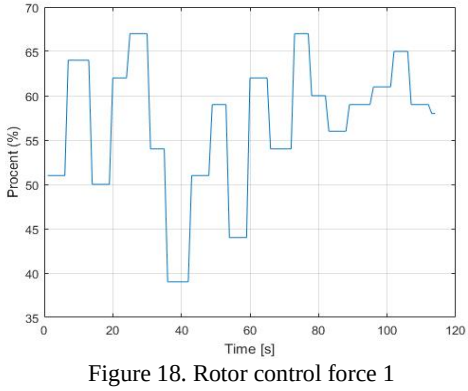

Figure 18. Rotor control force 1

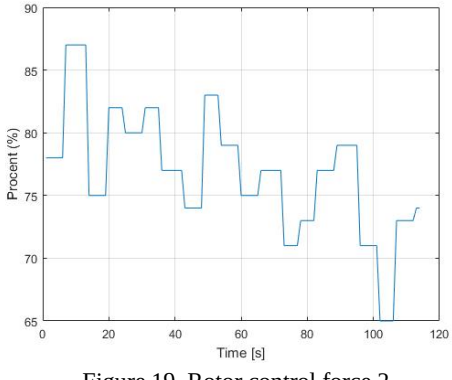

Figure 19. Rotor control force 2

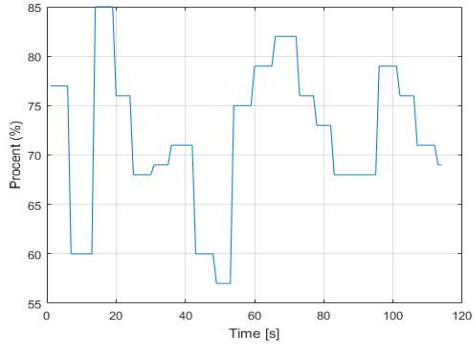

Figure 20. Rotor control force 4

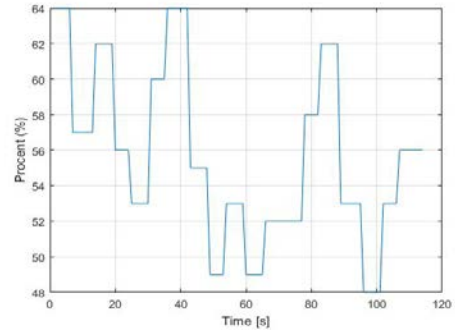

Figure 21. Rotor control force 4

c) Flight nr 184708 from 23.04.2019

For 10 seconds, the position deviations in meters were recorded (fig. 22), as well as the response in roll and pitch (fig. 23, 24).

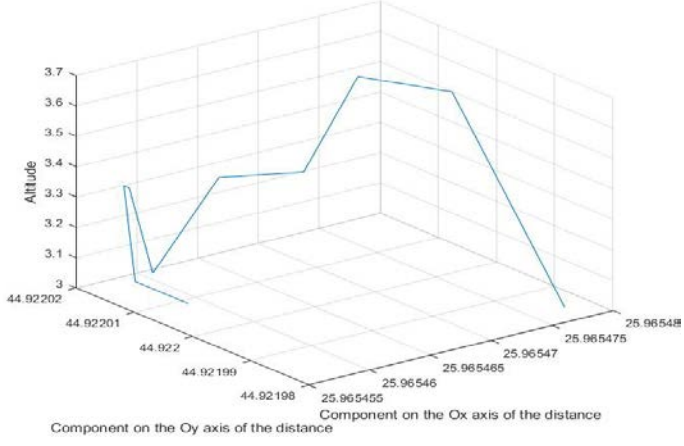

$\Delta x = 0{,}000019\text{m}$

$\Delta y = 0{,}00007\text{m}$

$\Delta z = 0{,}00001\text{m}$

Figure 22. Trajectory simulation case 3

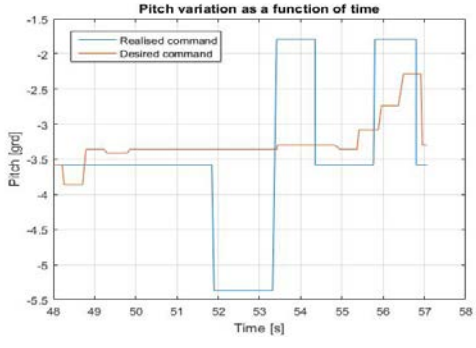

Figure 23. Pitch variation as a function of time

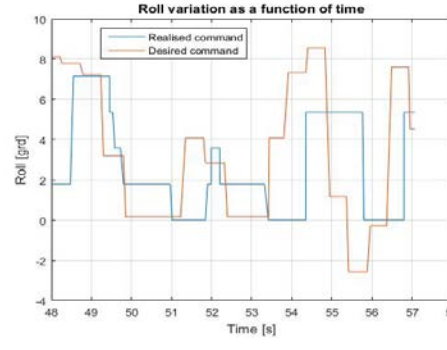

Figure 24. Roll variation as a function of time

The estimated delays in response to a pitch and roll command are as follows:
$T_{pitch} = 0{,}09$ s and $T_{roll} = 0{,}096$ s.

The percent values of the forces on each rotor were extracted from the database being shown in Fig. 25-28.

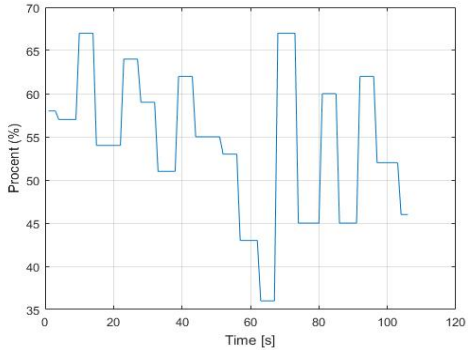

Figure 25. Rotor control force 1

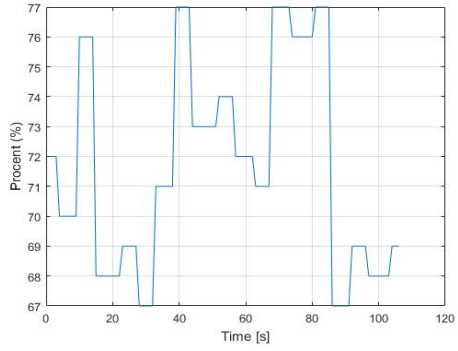

Figure 26. Rotor control force 2

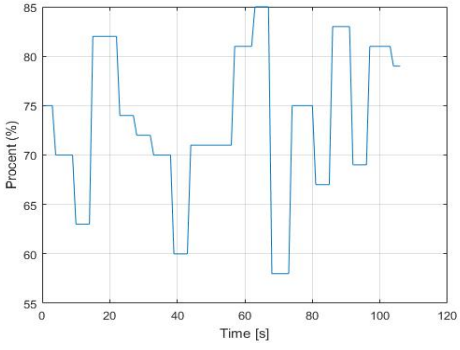

Figure 27. Rotor control force 3

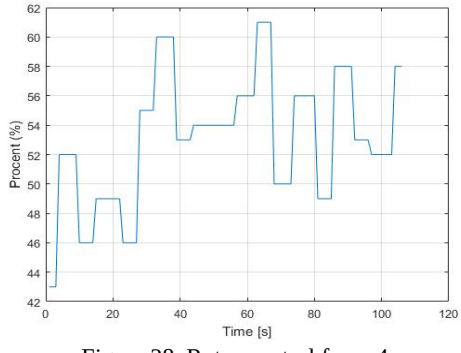

Figure 28. Rotor control force 4

The deviations in position at fixed point flight in the directions Ox, Oy and Oz are insignificant. In cases a) and b) the variations in height are due to the order made by the pilot.

Delays in response to a roll command are of the order of 0.09-0.94 sec and for the pitch command, the delays are of the order of 0.08-0.096 sec.

The control forces on each rotor are expressed as a percentage. The value of the hover forces are within permissible limits.

6. CONCLUSIONS

This paper presents the simulation and inflight experiment for the altitude and attitude control of the TWQH vehicle. Attitude control performances is of great importance, it is directly linked to the whole performances of the TWQH. The paper studied and implemented in the MicroPlot autopilot software the mathematical model of QH configuration, where the differential equation were derived form Newton – Euler formulation. The model was verified by simulating the hover phase of TWQH with the HORIZON simulator.

The main motivation is determined by the analysis of the results based on flying qualities requirements according to the UAV specifications.

We can see in above simulations and inflight tests that bounded oscillations in roll, pitch and yaw are inside of specific prescriptions. The altitude and attitude controller data were obtained in flight experiments, which keep the distance of the TWQH to the ground at desired value. The accuracy depends on the pilot action.

The experimental results obtained show that the proposed controller is able to stabilize the system even for relatively verified initial conditions due to atmospheric perturbation.

ACKNOWLEDGEMENT

This work [19] is a part of the "Unmanned platforms with dedicated capabilities and support infrastructure for national security mission applications" project contract no. 216/26.01.2017 under funds UEFISCDI, PNCDI III, programme 2, topic 2.1.

REFERENCES

[1] Z. Zuo, *Trajectory tracking control design with command-filtered compensation for a quadrotor*, Beijing, Nov 2009.
[2] B. Etkin, *Dynamics of flight*, John Wiley & Sons, New York, 1962.
[3] J. Roskam, *Airplane Flight Dynamics and Automatic Flight Controls: Part I., Part II.*, DARcorporation, Lawrence, Kansas, 2003.
[4] T. Hacker, *Stability and command in flight theory*, EA, 1968.
[5] * * * UAV platforms with dedicated capabilities and support infrastructure for applications in national security missions; Stage A; INCAS Technical report, Features of static and dynamic stability.
[6] * * * AAA33, *Advanced Aircraft Analysis User's Manual*, February 2011.
[7] * * * MIL F 8785B, *Military Specification: Flying Qualities of Piloted Airplanes*.
[8] * * * MIL-STD-1797, *Department of Defense Handbook: Flying Qualities of Piloted Aircraft*.
[9] * * * ADS – 33, *PRF Handling Qualities Requirements for Military Rotorcraft*.
[10] * * * *RTO-AVT UAV Design Processes and Criteria Structural Design Aspects and Criteria for Military UAV*.
[11] * * * MicroPilot – Horizon^{mp} User's Manual 3.7, Oct 2017.
[12] * * * MP2128$^{HELI/HELI2}$ Helicopter Autopilot User Manual, Oct 2018.
[13] D. Kotarski, Z. Benic, M. KRznar – Control design for unmanned aerial Vehicles with four rotors, *NDCS* **14**(2), 236-245,2016
[14] F. Sabatino, *Quadrotor control: nonlinear control design, and simulation modeling*, KTH, Stockholm, 2015
[15] H. M. Nabib ElKholy, *Dynamic modeling and control of a Quadrotoe Using Linear and Nonlinear Approaches*, AUC 2014.
[16] S. Bouabdallah, *Design and Control of Quadrotors with application to autonomous flying*, École Politechnique Fédérale de Lausanne, Feb 2007.
[17] T. Lukkonen, *Modelling and control of quadcopter*, Espoo, Aug 2011.
[18] J. Wang, F. Holzapfel, F. Peter, *Comparison of Nonlinear Dynamic Inversion and Backstepping Controls with Application to a Quadrotor*, Delft, Netherlands, April 2013.
[19] ** * * UAV platforms with dedicated capabilities and support infrastructure for applications in national security missions, Stage A*, INCAS Technical report, Aerodynamic design and analysis for UAV systems.